

68th Conference of the Italian Thermal Machines Engineering Association, ATI2013

Numerical Analysis of Air Flow Through Metal Foams

Andrea Diani^a, Kartik K. Bodla^b, Luisa Rossetto^{a*}, Suresh V. Garimella^b

^a*Dipartimento di Ingegneria Industriale, Università degli Studi di Padova, via Venezia 1, Padova 35131, Italy*

^b*School of Mechanical Engineering, Purdue University, 585 Purdue Mall, West Lafayette, IN 47907-2088, United States*

Abstract

X-ray micro computed tomography (μ -CT), originally developed for non-destructive biomedical imaging, is increasingly being employed in areas as diverse as materials characterization and reverse engineering. The technique employs computer processed X-rays to produce tomographic images or slices of specific regions of the object under investigation.

This paper presents a numerical analysis of air flow through four different high-porosity ERG copper foams having different pore sizes (5, 10, 20, and 40 pores per inch, PPI), and approximately the same relative density (6.4-6.6% solid fraction). These samples were scanned with a commercial micro computed tomography scanner at a resolution of 20 μ m, yielding a stack of two-dimensional images. Starting with these two-dimensional images, the real, random structure of the foams was reconstructed and subsequently meshed using the commercial software Simpleware. Meshes thus produced were then exported to FLUENT for simulating the fluid flow through the pore space of the foam samples. The results of μ -CT based CFD computations are compared against experimental measurements of pressure drop that were previously obtained with the same samples. The comparison reveals excellent agreement between the numerical and experimental results, highlighting the accuracy of this novel approach.

© 2013 The Authors. Published by Elsevier Ltd.

Selection and peer-review under responsibility of ATI NAZIONALE

Keywords: microtomography; metal foams; CFD; pressure drop; direct simulation

* Corresponding author. Tel.: +39 049 827 6869; Fax: +39 049 827 6896.

E-mail address: luisa.rossetto@unipd.it

1. Introduction

Metal foams are a class of cellular materials consisting of randomly oriented cells with nearly uniform sizes and shapes. They consist of a network of solid ligaments with interstitial pore spaces. Two morphologies exist for the metal foams: when the pores are interconnected with each other, the foam is called “open-cell foam”, whereas when most of the pores are isolated from one another, the resulting foam is known as “closed-cell foam”. Metal foams are primarily characterized by two parameters, *viz.*, the volumetric porosity denoted by ε , which is defined as the ratio of total void volume to cumulative volume occupied by the solid matrix and void space, and the number of pores per linear inch (PPI). Owing to their characteristics such as a large heat transfer area per unit of volume, and enhanced flow mixing capabilities, open-cell foams are gaining more attention for thermal management applications. For example, foams have been shown to be ideally suited for use in compact heat exchangers [1]. Specific details on experimental, analytical and numerical studies concerning fluid flow and thermal transport through such foams may be found in the literature [2-7].

Traditional approaches of modeling fluid and thermal transport through metal foams approximate stochastic foams as periodic porous materials, and employ a single unit cell for analysis. Lu et al. [8] developed a simple analytical model to evaluate the utility of metal foams as compact heat exchangers. A simple cubic cell model consisting of slender cylinders as edges was developed to capture the most important trends of energy flow due to forced convection, and conduction through cell ligaments of the cellular foam.

Boomsma et al. [9] modeled the fluid flow through porous media with periodic unit cells using the energy minimization tool, Surface Evolver [10]. The pressure drops from the numerical simulations were compared against previous experimental results [11]. Under identical conditions, it was reported that the pressure drop values predicted by the simulations were consistently approximately 25% lower than the experimental values, and this underestimation was attributed to the exclusion of wall effects in the simulations which would increase pressure drop.

Krishnan et al. [12] performed direct numerical simulation of thermal transport through open-cell foams using different periodic unit-cell geometries. They used three packaging arrangements of spheres, *viz.*, body centered cubic, face centered cubic and A15 lattice, to model the structure of the foams. Important thermal properties such as effective thermal conductivity, pressure drop and Nusselt number were computed for aluminum foams with both air and water as the interstitial fluid, and the results were successfully compared against experimental values and semi-empirical models from the literature.

There has been growing interest in the use of X-ray microtomography techniques for a variety of applications such as material characterization and reverse engineering. Bock and Jacobi [13] acquired detailed microtomography data of open-cell aluminum foams by employing X-ray micro computed tomography. Microstructure and morphology of four aluminum foam samples with 5, 10 and 20 PPI were analyzed in detail. The image analysis revealed the strut cross section of the foam ligaments to be triangular, and not circular as was assumed in most prior works. The data also showed a large variation in strut size, which highlighted the irregularity of the metal foam structure. Similar observations were also noted in Bodla et al. [14].

Micro computed tomography images may also be employed as the starting point for a CFD analysis. Metal foams are inherently stochastic; thus, unit-cell based models only approximate the true microstructure and fail to capture the intricate details of fluid flow and heat transfer in such media. Recent advancements in computing architecture have led to increased processor speeds and memory, which enable tomography scans to be employed for mesh generation and subsequent, detailed fluid-thermal performance analysis of random porous materials such as metal foams. Bodla et al. [15] adopted this approach to compute heat transfer and fluid flow parameters for aluminum foams of varying PPI. The numerical results for thermal conductivity, permeability, friction factor and heat transfer coefficient were compared against experimental values and empirical correlations from the literature.

In the present study, a numerical investigation of fluid flow through the real structure of four different copper foams, having about the same relative density (6.4 – 6.6%) but different pore sizes (5, 10, 20, and 40 PPI) is performed. The real structures are reconstructed from micro computed tomography images obtained at a scanning resolution of 20 μm . The hydraulic behavior thus computed is compared against experimental pressure drop values previously obtained on the same four copper foams.

2. Methodology

Computed tomography was first applied as a medical imaging procedure that uses computer-processed X-rays to produce tomographic images or slices of specific areas of the body. The two-dimensional images can be combined to produce a three-dimensional image, and may thus be employed for diagnostic or therapeutic purposes in various medical disciplines.

During the 1970s, computed tomography applications spread to industrial problems. Industrial CT scanning is now used in many areas for a variety of applications such as internal inspection of components for flaw detection, failure analysis, metrology, reverse engineering, and materials characterization. In this study, the computed tomography technique is employed for scanning four different copper foam samples, whose main characteristics are reported in Table 1; t represents the fiber thickness, l the fiber length, and a_{sv} the total available heat transfer area per unit of volume.

Table 1. Geometrical characteristics of the four copper foam samples.

Sample	PPI [item in ⁻¹]	Porosity [-]	t [mm]	l [mm]	a_{sv} [m ² m ⁻³]
Cu-5-6.5	5 ^a	0.935 ^a	0.495 ^b	1.890 ^b	292 ^a
Cu-10-6.6	10 ^a	0.934 ^a	0.432 ^b	1.739 ^b	692 ^a
Cu-20-6.5	20 ^a	0.935 ^a	0.320 ^b	1.402 ^b	1134 ^a
Cu-40-6.4	40 ^a	0.936 ^a	0.244 ^b	0.999 ^b	1611 ^a

^a Measured by the manufacturer [16]

^b Measured by Mancin et al. [17]

All of these foams are manufactured in a sandwich-like arrangement, where the foam core height is brazed between two 10 mm thick copper plates. Experimental specimens were 100 mm long and wide and 40 mm high, and were previously tested by Mancin et al. for their pressure drop and heat transfer performance [17]. In that study, the authors characterized the air flow through 21 foams samples, which includes the four samples under investigation in this work. They analyzed and discussed how the various geometrical parameters of these enhanced surfaces affect the thermal and fluid flow behavior.

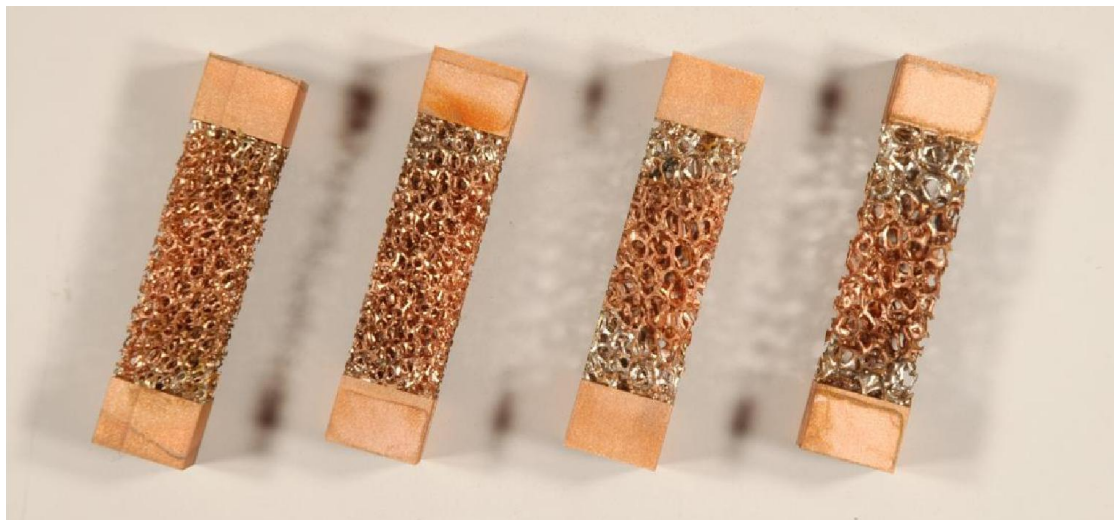


Fig. 1. Copper foam slabs (40, 20, 10, and 5 PPI, respectively).

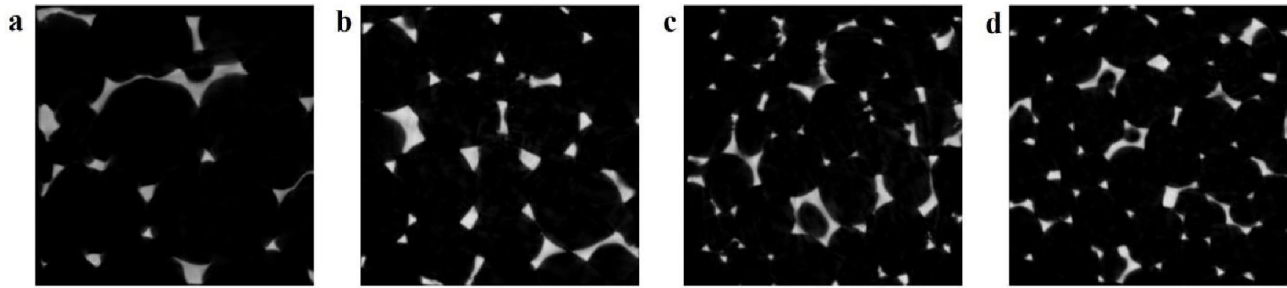


Fig. 2. Representative two-dimensional scan images shown for: (a) 5 PPI, (b) 10 PPI, (c) 20 PPI, (d) 40 PPI, respectively.

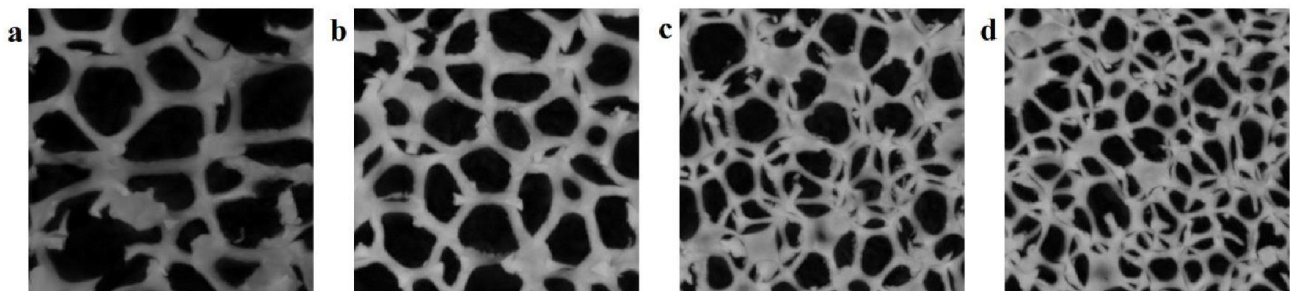


Fig. 3. Examples of the reconstructed foams. Images correspond to: (a) 5 PPI, (b) 10 PPI, (c) 20 PPI, (d) 40 PPI, respectively.

Owing to a trade-off between scan resolution and size of the sample being scanned, smaller samples were used in the scanning and subsequent numerical analysis. For this purpose, square specimens with an edge size of 15 mm were cut from the original copper samples by means of electro-erosion. This cutting technique avoids damage to the fiber ligaments, and hence the structure is scanned without introducing any defects. The cut foams, shown in Fig. 1, were scanned with a commercial X-ray μ -CT scanner at a resolution of 20 μ m, with the axis along the longer direction, *i.e.*, along the height of the foams. This resolution was chosen to enable all the microstructural details of the individual pores and ligaments to be captured.

The image processing was performed with the commercial software Simpleware [18] employing the ScanIP module, which permits operations such as filtering, noise removal, region identification, and three-dimensional reconstruction. It also permits exporting the 3D images for CAD or mesh generation. In Fig. 2, examples of the scan images are shown for the 5, 10, 20, and 40 PPI copper foams. The strut cross sections seem to be mostly triangular, as also observed by Bock and Jacobi [13]. The demarcation between the solid phase and the fluid phase is not crisp: metal absorbs X-rays leading to brighter zones, whereas air let X-rays pass, leading to darker zones. Thus, the identification of the two distinct regions (fluid and solid) is based on a threshold value. Appropriate greyscale values are identified so as to match the porosities of the reconstructed foams with those provided by the manufacturer. Further, floodfill segmentation was also performed to retain the connected ligaments, while discarding the unconnected loose ones.

At this point, since a large number of pixels would increase both the number of mesh elements and the demand on memory, a down-sampling operation was performed, such that the resolution of images is slightly lowered but the geometry is still well-represented. Representative reconstructions of the foam samples are shown in Fig. 3. According to the measurements reported in Table 1 and as can be seen from Fig. 3, the pores become smaller and the ligaments shorter and thinner as the number of pores per linear inch of the sample increases.

The foam region in the brazed regions adjacent to the copper plates at the bottom and top (see Fig. 1) was difficult to reconstruct as the presence of the copper plate created considerable noise in the scanned images. As a result, it was not possible to reconstruct the entire height of the scanned samples (40 mm). The typical reconstructed sample height was roughly 30 mm, omitting 5 mm of interface region on either side. However, this height is sufficient for fluid flow computations, as will be explained in the following section.

3. Numerical model

The reconstructed three-dimensional foams are input to the ScanFE module in Simpleware [18] for generating finite-volume meshes. Meshing the entire scanned volume would place a significant demand on memory during mesh generation. Further, the meshes thus produced would need huge computational resources for numerical analysis of fluid flow. Therefore, only smaller regions were employed for mesh generation. The length of the sample in the flow direction was 100 mm in the experiments, leading to fully developed flow. To ensure similar, fully developed flow conditions in the numerical simulations, the foam must have an adequate number of pores in the flow direction. A sensitivity analysis was carried out in order to determine the number of pores that is necessary for attaining fully developed flow. Preliminary simulations were run on the 40 PPI sample with fluid domains having the same boundary conditions and fluid properties but different number of pores along the flow direction. Domains consisting of 5, 10, and 20 pores in the flow direction were considered, and the difference in the pressure gradient determined. It was observed that the difference in pressure gradient between the 10 pore and the 5 pore sized domains was -15.7%, whereas between the 20 pore and 10 pore sized domains, the difference was only -3.2%. A domain size of approximately 10 pores in the flow direction is therefore deemed sufficient for the flow to attain fully developed conditions for the flow speeds considered for the 10, 20, and 40 PPI samples. However, for the 5 PPI copper foam, only 6 pores were present in the flow direction as the maximum height that was possible to reconstruct was only 30 mm, as described in the previous section.

At a constant minimum mesh element size, and considering domains with 10 pores along the flow direction, the number of mesh elements directly depends on the number of pores per linear inch of the foam; the number of mesh elements increases when linear porosity decreases because the pore dimension increases, and *vice-versa*. To reduce the overall mesh count, mixed tetrahedral and hexahedral elements were employed during meshing. Table 2 presents the size of the meshed domain along with the number of elements present in the meshed volume.

Table 2. Domain sizes and number of mesh elements in a typical volume employed for analysis.

Sample	Size [mm×mm×mm]	N° mesh elements
Cu-5-6.5	9.92×9.92×29.96	~27 million
Cu-10-6.6	5.96×5.96×25.36	~10 million
Cu-20-6.5	4.40×4.80×12.76	~5 million
Cu-40-6.4	4.48×4.48×6.34	~3 million

Considering a pore diameter of 5.08, 2.54, 1.27, and 0.635 mm for the 5, 10, 20, and 40 PPI foam, respectively, 10 pores are included along the flow direction for all the samples, except for the 5 PPI sample for which 6 pores are included. The meshes are created with the ScanFE module of Simpleware [18] as noted previously.

The continuity and momentum equations for a laminar steady-state incompressible flow are given by:

$$\frac{\partial}{\partial x_i} \rho u_i = 0 \quad (1)$$

$$\frac{\partial}{\partial x_i} (\rho u_j u_i) = -\frac{\partial P}{\partial x_i} + \frac{\partial}{\partial x_i} \left(\mu \frac{\partial u_i}{\partial x_j} \right) \quad (2)$$

where u represents the air velocity in the i or j direction, ρ the density of fluid and μ the dynamic viscosity. The governing equations are solved using the finite-volume commercial software ANSYS Fluent [19], using a first-order upwind difference scheme for flow calculations. The SIMPLE scheme is employed for pressure-velocity coupling, and the flow field is deemed converged when the absolute value of all the residuals falls below 1.0×10^{-6} .

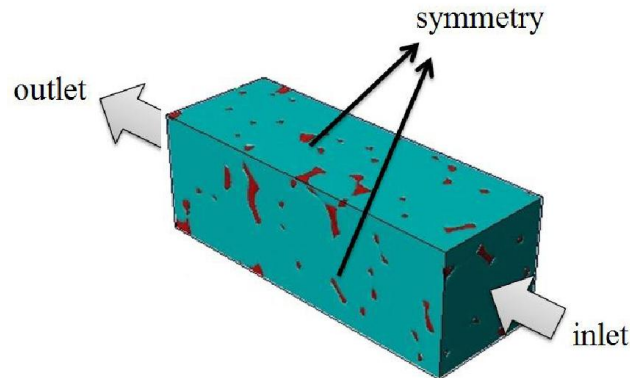


Fig. 4: Boundary conditions employed in the present study.

The boundary conditions employed in the present work are shown schematically in Fig. 4. Here, the solid zone is highlighted in red, while the fluid zone is shown in blue. The boundary conditions are also detailed below:

- velocity-inlet boundary condition at the inlet of the fluid domain;
- pressure-outlet boundary condition at the outlet of the fluid domain;
- symmetry boundary conditions on the lateral sides of the domain; and
- wall with no slip boundary condition on the interface between the solid and fluid domains.

The flow is assumed to be three-dimensional, steady-state and incompressible, and the working fluid is air, with constant fluid properties calculated at the mean values of air temperature and pressure as reported in [17]. Further, simulations were only performed in the laminar regime, with Reynolds numbers (based on the superficial velocity and on the square root of permeability [15] as the characteristic length) in the range of 62 – 215. The following section presents the details of the results obtained, as well as a comparison against experiments.

4. Numerical results

The experimental velocities and air properties [17] are taken as input parameters for the numerical simulations, to enable a direct comparison. A superficial velocity range of 2.5 to 5 m s⁻¹ is explored in the numerical study, with the air being at ambient pressure as in the experiments. For each sample, 6 different velocities are investigated, and the resulting numerical pressure gradients are compared against the corresponding experimental values.

In Fig. 5, the numerical pressure gradients for the 4 copper foams are plotted against the pore velocity. It is observed that the pressure gradient has an almost quadratic dependence on velocity in the range of the tested working conditions, in accordance with the Darcy-Forchheimer equation. At any velocity, the samples with the smallest pore sizes (or largest PPI) demonstrated the highest pressure drop and *vice-versa*, as expected. Similar observations may also be made from the experimental results of Mancin et al. [17].

Fig. 6 compares pressure gradients from the numerical simulations against data from experiments performed at similar velocities. The pressure gradient results for the four copper foams are seen to match the experimental values very well, globally with a mean relative and absolute deviation of -3.8% and 5.4%, respectively. Relative, absolute, and standard deviations between the numerical and experimental results for each foam are summarized in Table 3. This validates the numerical approach employed in the present study and demonstrates the utility of the employed approach in computing detailed flow physics directly at the pore scale. Currently, we are in the process of extending this analysis to include convective heat transfer computations.

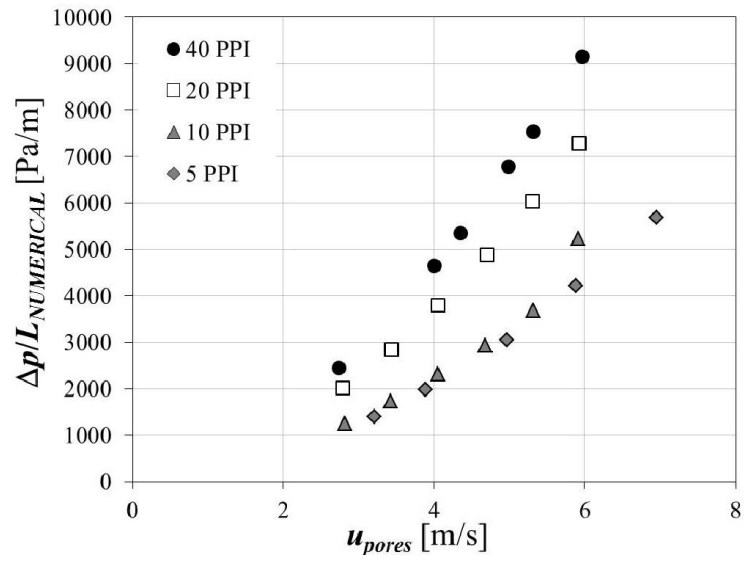


Fig. 5. Numerical pressure gradient plotted against the pore velocity.

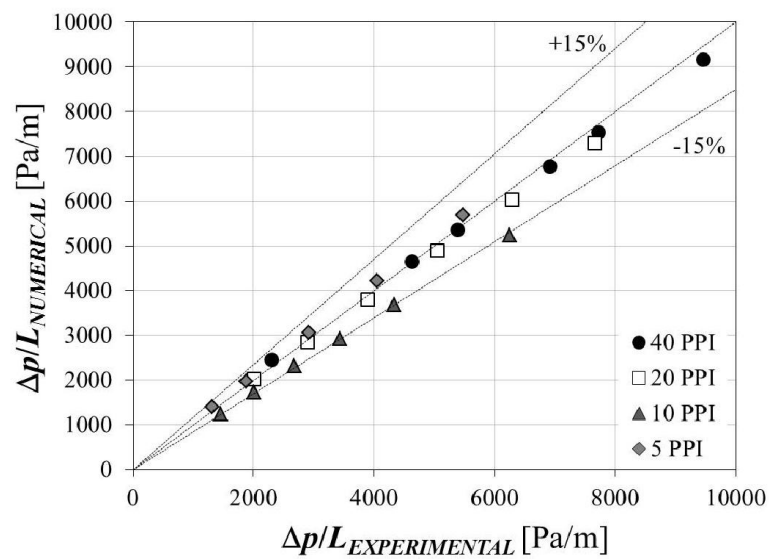


Fig. 6. Comparison between numerical and experimental pressure gradients.

Table 3. Difference between numerically computed and experimental pressure gradients, shown for the four copper foams considered.

Sample	dev _{rel} [%]	dev _{abs} [%]	σ _{std} [%]
Cu-5-6.5	2.1	2.2	1.9
Cu-10-6.6	-14.6	14.6	0.6
Cu-20-6.5	-2.7	2.8	1.6
Cu-40-6.4	-0.4	2.4	1.9

5. Conclusions

Air forced convection of air through the real structure of metal foams is numerically investigated. Pore-scale structures are obtained by micro-computed tomography scanned images of four different copper foams, having about the same relative density (6.4 – 6.6%) but different linear porosity (5, 10, 20, and 40 PPI), with a scan resolution of 20 μm . The scanned samples were reconstructed and meshed employing the commercial software, Simpleware.

Fluid flow simulations were performed using the commercial software ANSYS Fluent, and experimental conditions reported in a previous work were considered as boundary conditions for the present numerical study to facilitate direct comparison. Pressure gradients are found to have a quadratic dependence on velocity in the simulated test conditions. Further, the pressure gradient increases as the number of pores per inch increases. It was observed that the numerical analysis employed in this study predicts pressure gradients very well - pressure gradients are estimated to within $\pm 5\%$ for the 5, 20, and 40 PPI samples, whereas pressure gradients for the 10 PPI sample are underestimated by about 15%, relative to experimental data. This validates the analysis procedure which can now be extended to predict thermal performance of random metal foams.

Acknowledgement

The support of the MIUR through the PRIN Project 2009TSYPM7_003 is gratefully acknowledged.

References

- [1] Zilio C, Mancin S, Diani A, Rossetto L. Aluminum foams as possible extended surfaces for air cooled condenser. International Congress of Refrigeration. Prague. 2011:ICR2011-B2-566.
- [2] Zhao CY. Review on thermal transport in high porosity cellular metal foams with open cells. Int J Heat Mass Transfer 2012;55:3618-3632.
- [3] Mahjoob S, Vafai K. A synthesis of fluid and thermal transport models for metal foam heat exchangers. Int J Heat Mass Transfer 2008;51:3701-3711.
- [4] Annapragada SR, Murthy JY, Garimella SV. Permeability and Thermal Transport in Compressed Open-Celled Foams. Numerical Heat Transfer, Part B: Fundamentals 2008;54:1-22.
- [5] Mancin S, Zilio C, Diani A, Rossetto L. Experimental air heat transfer and pressure drop through copper foams. Exp Thermal Fluid Science 2012;36:224-232.
- [6] Ribeiro GB, Barbosa Jr JR, Prata AT. Performance of microchannel condensers with metal foams on the air-side: Application in small scale refrigeration systems. Applied Thermal Engineering 2012;36:152-160.
- [7] Gibson LJ, Ashby MF. Cellular solids-structures and properties. Cambridge Solid State Science Series, second ed. Cambridge University Press 1997.
- [8] Lu TJ, Stone HA, Ashby MF. Heat transfer in open-cell metal foams. Acta mater 1998;46:3619-3635.
- [9] Boomsma K, Poulikakos D, Ventikos Y. Simulations of flow through open cell metal foams using an idealized periodic cell structure. Int J Heat Fluid Flow 2003;24:825-834.
- [10] Brakke K. The Surface Evolver. Experimental Mathematics 1992;1:141-165.
- [11] Boomsma K, Poulikakos D. The effects of compression and pore size variations on the liquid flow characteristics of metal foams. J Fluids Eng 2002;124:263-272.
- [12] Krishnan S, Garimella SV, Murthy JY. Simulation of thermal transport in open-cell metal foams: Effects of periodic unit-cell structure. J Heat Transfer 2008;130:024503-1-5.
- [13] Bock J, Jacobi AM. Geometrical classification of open-cell metal foams using X-ray micro-computed tomography. Materials Characterization 2013;75:33-43.
- [14] Bodla KK, Murthy JY, Garimella SV. Resistance network-based thermal conductivity model for metal foams. Computational Material Science 2010;50:622-632.
- [15] Bodla KK, Murthy YM, Garimella SV. Microtomography-based simulation of transport through open-cell metal foams. Numerical Heat Transfer, Part A 2010;58:527-544.
- [16] ERG Material and Aerospace Inc. Auckland CA. Web site www.ergaerospace.com.
- [17] Mancin S, Zilio C, Diani A, Rossetto L. Air forced convection through metal foams: Experimental results and modeling. Int J Heat Mass Transfer 2013;62:112-123.
- [18] Simpleware Ltd. 2012. Exeter, UK.
- [19] ANSYS Fluent 13. 2010.